



Elucidation of the photoinduced transformations of Aliskiren in river water using liquid chromatography high-resolution mass spectrometry

Nuno P.F. Gonçalves^a, Lucia Iezzi^a, Masho H. Belay^b, Valeria Dulio^c, Nikiforos Alygizakis^{e,f}, Federica Dal Bello^d, Claudio Medana^d, Paola Calza^{a,*}

^a Department of Chemistry, University of Turin, Torino, Italy

^b Department of Science and Technological Innovation, University of Piemonte Orientale, Alessandria, Italy

^c INERIS, National Institute for Environment and Industrial Risks, Verneuil en Halatte, France

^d Department of Molecular Biotechnology and Health Sciences, University of Turin, Torino, Italy

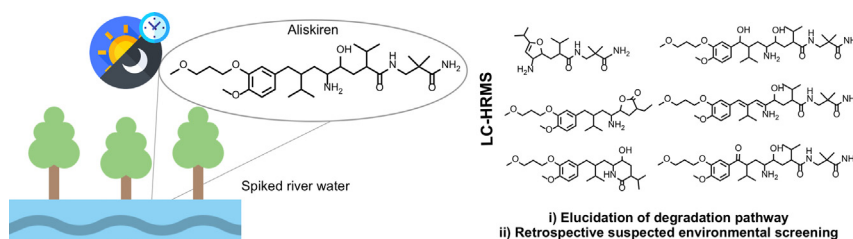
^e Laboratory of Analytical Chemistry, Department of Chemistry, University of Athens, Panepistimiopolis Zografou, 15771 Athens, Greece

^f Environmental Institute, Okružná 784/42, 97241 Koš, Slovak Republic

HIGHLIGHTS

- The environmental fate of aliskiren was investigated in spiked river water.
- Indirect and direct photolysis plays a key role in the drug fate.
- Degradation mechanism has been proposed based on photoproducts' structures.
- Environmental occurrence of two TPs was confirmed at by retrospective analysis.
- In silico bioassays suggest the formation of TPs with distinct toxicity.

GRAPHICAL ABSTRACT



ARTICLE INFO

Article history:

Received 27 May 2021

Received in revised form 16 July 2021

Accepted 5 August 2021

Available online 8 August 2021

Editor: Dimitra A Lambropoulou

Keywords:

HRMS

Aliskiren

Toxicity

Transformation products

Environmental fate

ABSTRACT

Aliskiren was selected as a compound of potential concern among a suspect screening list of more than 40,000 substances on a basis of high occurrence, potential risk and the absence of information about its environmental fate.

This study investigated the photoinduced degradation of aliskiren in river water samples spiked at trace levels exposed to simulated sunlight. A half-life time of 24 h was observed with both direct and indirect photolysis playing a role on pollutant degradation. Its photo-induced transformation involved the formation of six transformation products (TPs), elucidated by LC-HRMS - resulted from the drug hydroxylation, oxidation and moieties loss with subsequent cyclization structurally. The retrospective suspected analysis performed on a total of 754 environmental matrices evidenced the environmental occurrence of aliskiren and two TPs in surface waters (river and seawater), fresh water, sediments and biota. In silico bioassays suggested that aliskiren degradation undergoes through the formation of TPs with distinct toxicity comparing with the parent compound.

© 2021 The Authors. Published by Elsevier B.V. This is an open access article under the CC BY license (<http://creativecommons.org/licenses/by/4.0/>).

1. Introduction

The public awareness about the impact of human activities on water quality is constantly growing and is now considered one of the major global concerns for the future decades (Naciones Unidas, 2018). Urban

* Corresponding author.

E-mail address: paola.calza@unito.it (P. Calza).

runoff and poorly effective wastewater treatment plants are continuously releasing many chemicals into the environment. Aqueous ecosystems are therefore the ultimate destination for a large group of pollutants, the so-called contaminants of emerging concern (CECs), with the potential to pose ecological and public health hazards.

CECs include pharmaceuticals, personal care products, pesticides, hormone disrupting substances, *per*- and polyfluoroalkyl substances (PFAS), etc. (Diamanti et al., 2020; Ebele et al., 2017; Miller et al., 2018; Patel et al., 2019). These pollutants are non-regulated, not included in the daily routine water analysis and without information about their potential hazard for the aquatic biota and humans (von der Ohe and Dulio, 2013). Because of the persistence, bioactivity and bioaccumulation potential of several of these substances, the concern is increasing about the possible harmful effects on aqueous ecosystems and human health (Alygizakis et al., 2020; Hollender et al., 2019; Miller et al., 2018).

Once released in the aquatic environment, pollutants may undergo several transformations such as hydrolysis, microbial degradation, interactions with dissolved organic matter, and photodegradation. Thus, it is important to study the pollutants environmental fate by evaluating the formation of their transformation products (TPs) and their ecotoxicological properties. Photoinduced reactions occurring in surface waters comprise direct and indirect photolysis. Direct photolysis involves sunlight absorption by the pollutant with its transformation, while during indirect photolysis photoactive compounds absorbed sunlight. In the last one, dissolved organic matter (DOM), nitrite and nitrate can generate reactive species, such as the hydroxyl radical ($\cdot\text{OH}$), singlet oxygen ($^1\text{O}_2$) and DOM triplet states (^3DOM), capable to react with pollutants (Berg et al., 2019; Bodrato and Vione, 2014; Luo et al., 2021; Ma et al., 2021).

The increasing number of new medicines together with their extensive use, persistence and high biological activity placed pharmaceuticals as the CECs epicenter. Even if most of the pharmaceuticals are not highly persistent, their continuous release into the environment which is significantly fast than the environmental degradation rate allows to categorize them as “pseudo-persistent” (Bu et al., 2016). Among pharmaceuticals, antihypertensive drugs, including beta-blockers, are pointed as one of the most frequently detected drug classes in the environment (Godoy et al., 2015; Stankiewicz et al., 2015), representing 12% of total therapeutics (Santos et al., 2010). Several studies linked these substances to several disorders such as reduced growth rates, reduction in its heart rate, decreased egg production and reproduction on non-target organisms such as fish (*Japanese medaka*, *rainbow trout*), invertebrates (*Daphnia magna*, *Hyalella azteca*, *Daphnia lumholzi*, *Ceriodaphnia dubia*), and green algae (*Pseudokirchneriella subcapitata*) (Maszkowska et al., 2014; Santos et al., 2010).

Aliskiren is a direct renin inhibitor used in the treatment of hypertension, widely used since 2009 as a monotherapy or as the principal component of as many as eight aliskiren-based drug combinations (Duggan et al., 2010), with a daily prescription of 150 - 300 mg, and it is mainly eliminated in the unmetabolized form ($79.8 \pm 3.0\%$) (Waldmeier et al., 2007). As a result, aliskiren is one of those CECs continuously released in water that has been detected in the aquatic environment (“NORMAN Database System”). As example, Singer et al., 2016, investigating the occurrence of pharmaceuticals in wastewater treatment plants effluents reported the presence of aliskiren drug in all samples from concentrations ranging from 0.4 up to $1.9 \mu\text{g L}^{-1}$. Gago-Ferrero et al., 2020 evidenced the inefficiency of the wastewater treatment processes to remove aliskiren, with a slightly decrease from $0.27 \mu\text{g L}^{-1}$ (influent) to $0.25 \mu\text{g L}^{-1}$ (effluent). Additionally, Boulard et al., 2020, reported concentrations ranging from 0.4 up to 5.0 ng L^{-1} following the drug in the Rhine River (Germany) during period 2005–2015, immediately after the commercial approval finding a correlation with the consumption trends data. Despite their presence in environmental matrices, to the best of our knowledge there is no information about aliskiren environmental fate.

In this work, we investigated for the first time the photoinduced transformation of aliskiren in aqueous milieu by identifying its transformation products via LC-HRMS. We exposed river water samples spiked with aliskiren at $\mu\text{g L}^{-1}$ level to simulated sunlight for assessing sunlight-induced photolysis. The contribution of direct and indirect photolysis was then unraveled by exposing aliskiren to irradiation in ultrapure water or in the presence of humic acid substances and nitrate. TPs formation in the natural environment was then confirmed by applying a retrospective analysis and their potential toxicity was explored by *in-silico* studies.

2. Materials and methods

2.1. Chemicals

Aliskiren (CAS: 173334-57-1) purity $\geq 98\%$, was purchased from Sigma-Aldrich (Milan, Italy) and its structure is shown in Fig. 1. Humic acid sodium salts (technical, 50–60% as HA) from Aldrich-Chemie (Milan, Italy). Sodium nitrate (analysis grade) was purchased from Merck, KGaA. All the chemical reagents were used as received. Suspensions and standard solutions were prepared in ultrapure water.

The real river water was sampled in River Po, Torino Italy (September, 14th 2020). After a pre-filtration step, with a grade qualitative filter paper (Whatman) sample was passed through a hydrophilic $0.45 \mu\text{m}$ filter Sartolon Polyamide (Sartorius Biolab). Sample analysis showed a total organic carbon = 1.92 mg L^{-1} , inorganic carbon = 44.60 mg L^{-1} , total nitrogen = 3.940 mg L^{-1} and a pH = 8.2. HRMS analyses of river water sample showed that aliskiren, its identified TPs and the known metabolites were below the detection limit.

2.2. Methods

2.2.1. Photolysis experiments

The degradation experiments were performed in 200 mL of ultrapure and river water samples spiked with aliskiren ($5 \mu\text{g L}^{-1}$). Water samples were distributed into three Pyrex glass cells (7.5 cm height \times 9.5 cm diameter) and exposed to a sunlight simulator (Solarbox, CO.FO.Me.Gra, Milan) equipped with a xenon lamp (1500 W) with a cut-off filter at below 340 nm, during times ranging from 1 h to 72 h. On top of the suspensions the irradiance was 18 W m^{-2} in the 295 – 400 nm range (analogous to the natural sunlight UV irradiance at middle European latitude in sunny days) (Bodrato and Vione, 2014). Dark experiments were conducted protecting the samples from light. Degradation experiments were also performed in the presence of humic acid and nitrate at a final concentration of 2 mg L^{-1} . Samples were freeze-dried (LABOGENE – CoolSafe 55-110) and then dissolved in 5 mL of acetonitrile and 5 mL of methanol and filtered with a $0.22 \mu\text{m}$ polypropylene filter (ThermoFisher Scientific). Before the analysis by LC-HRMS, the samples were dried at room temperature under a gentle N_2 stream and reconstituted with 200 μL of acetonitrile (pre-concentration of 1000). The degradation experiments were carried out in duplicated, the results averaged and the error bars ($\pm\sigma$) reported in the relevant plots. The repetitions showed high robustness and reproducibility of the adopted experimental procedures.

2.2.2. Analytical procedures

Aliskiren disappearance and the formation of TPs formation analyses were performed using an Ultimate 3000 HPLC with a LTQ-orbitrap mass spectrometer (Thermo Scientific, Bremen, Germany) operated in ESI mode. Analyses were performed by injecting 20 μL in a column C18 (Luna(2) C18, $150 \times 2 \text{ mm}$, $3 \mu\text{m}$, 110 \AA ; Phenomenex, Castel Maggiore, BO, Italy) using the mixture acetonitrile and formic acid solution (20 mM) as eluent with the following gradient: 0 min, 95:5 v/v; 18 min, 60:40 v/v; 23 min, 0:100 v/v; then the column was reconditioned (flow rate 0.2 mL/min).

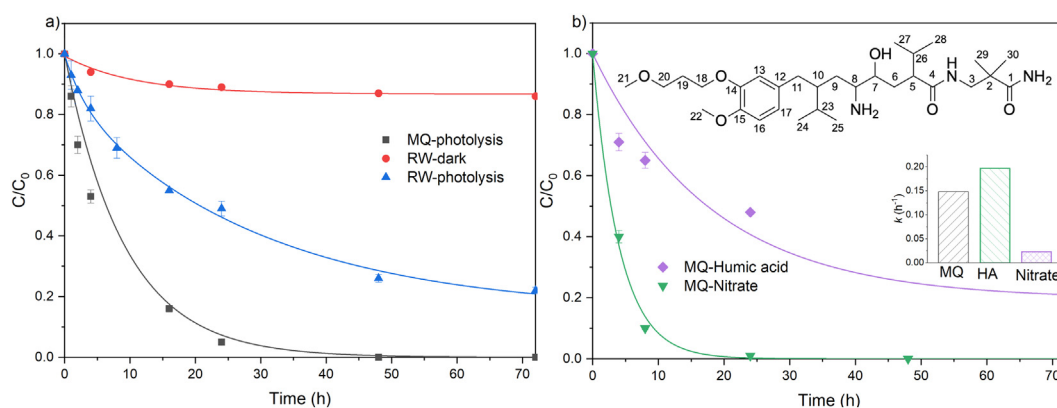


Fig. 1. Degradation of aliskiren, a) in ultrapure water (MQ-black line) and river water (RW-blue line) under irradiation and in the absence of light (red line); b) in the presence of humic acid and nitrate. Inset: first-order kinetic constants; numbering of aliskiren carbon atoms.

The ESI ion source used N_2 as sheath and auxiliary gas. Source parameters were the following: sheath gas 30 arbitrary unit (arb); auxiliary gas 25 arb; capillary voltage 4.0 kV and capillary temperature 275 °C. Full mass spectra were acquired in positive ion modes using a m/z range between 50 and 500; resolution was set at 30,000. MS^n spectra were acquired in the range between ion trap cut-off and precursor ion m/z values. Accuracy on analyzed m/z (versus calculated) was ± 0.001 (without internal calibration).

Total organic carbon (TOC) and total nitrogen (TN) analyses were performed in a Shimadzu TOC-5000 analyzer (catalytic oxidation on Pt at 680 °C) using standards of potassium phthalate for the calibration.

2.2.3. In silico studies

In silico ecotoxicity assessments were performed using the VEGA QSAR software (<https://www.vegahub.eu/>, version 1.1.5 beta 48) developed by Politecnico di Milano, Italy (Benfenati et al., 2013). VEGA is a quantitative structure-activity relationship (QSAR) platform to predict toxicity based on different models supported on the OECD principles for acceptance of QSAR models for regulatory use. Mutagenicity (AMES test) simulations were carried out by the CONSENSUS model (v 1.0.3) of four tests (KNN – version 1.0.0; SarPy – version 1.0.7; ISS – version 1.0.2 and CAESAR – version 2.1.13). The toxicity tests for *Fathead minnow* LC_{50} (96 h) and *D. magna* LC_{50} (48 h) were performed using the EPA model (version 1.0.7) based on T.E.S.T. software (US EPA) while the tests for Fish acute toxicity (LC_{50}) were performed by the toxicity NIC model (version 1.0.0).

2.2.4. Retrospective suspected screening

For retrospective analysis, Digital Sample Freezing Platform (DSFP) was used, which is a platform developed by the NORMAN Association to store environmental samples (Alygizakis et al., 2019b). The samples can be retrospectively screened for environmentally relevant substances uploaded to the NORMAN Substance Database (SusDat) (Network et al., 2020; NORMAN Database System, 2020). Each laboratory aims to create its own collection of digitally archived chromatograms. For the purpose of this study, digitally archived environmental samples provided by the National and Kapodistrian University of Athens (Greece) and Environmental Institute (Slovakia) were used to perform the retrospective analysis. The samples were analyzed by a UHPLC device (Dionex UltiMate 3000 RSLC from Thermo Fisher Scientific) coupled to a Bruker Maxis Impact QTOF-MS/MS analyzer (Bremen, Germany). The chromatographic separation was achieved using an Acclaim RSLC C18 column (2.1×100 mm, $2.2 \mu m$), preceded by an ACQUITY UPLC BEH C18 $1.7 \mu m$ pre-column (Waters, Ireland). The analytical column and the pre-guard column were thermostated at 30 °C during separation. The samples were analyzed using two acquisition modes: broadband collision-induced dissociation (bbCID, data-

independent) and 5 most abundant AutoMS acquisition (data-dependent) in positive ionization. Instrumental parameters are described elsewhere (Gago-Ferrero et al., 2020). A total of 754 environmental samples were investigated for the occurrence of the parent drug aliskiren and the five elucidated TPs through retrospective suspect screening (Alygizakis et al., 2019b). The list of the samples that were searched is provided in the Table S2 (see supplementary information material). For each batch of samples at least one procedural blank sample was included for quality assurance (in total 37 procedural blanks). Most of the samples were collected in national and international monitoring campaigns such as joint Danube survey 4 (JDS4) (Alygizakis et al., 2019a; Liška et al., 2021), river monitoring campaigns (e.g. Donets/Dniester/Dnieper) (Diamanti et al., 2020), monitoring of the Black Sea (EMBLAS-II) (Slobodnik et al., 2017), monitoring of top predators and their prey from specimen banks in context of LIFE APEX among others. The data files were converted to open-source format (mzML) using Bruker CompassXport 3.0.9.2. (Bremen, Germany) and were uploaded to NORMAN Digital Sample Freezing Platform (DSFP) (Alygizakis et al., 2019b) together with their meta-data. DSFP processes the mzML with a non-target screening workflow involving centWave for peak picking (Tautenhahn et al., 2008) using previously optimized ppm and peakwidth parameters (Libiseller et al., 2015) and componentization (grouping adducts and isotopic peaks) (Loos et al., 2012). The final output is a component list, which can be searched for any suspected compound by suspect screening given the analytical limitations in extraction and ionization. Therefore, the data can be screened for a 'yes/no' presence of virtually any compound amenable to LC-MS analysis using a combination of information on its (i) exact mass (< 2 mDa), (ii) predicted retention time window in the chromatogram (20% retention time range), (iii) isotopic fit ($> 90\%$ using MOLGEN (Meringer and Schymanski, 2013) if available) (iv) qualifier fragment ions (at least two qualifier fragment ions). TPs that fulfilled the identification criteria were considered to be present in the samples. Regarding screening detection limit (SDL), they proved to be 1.00 ng L^{-1} for ground water, 1.25 ng L^{-1} for surface water, 2.0 ng L^{-1} for wastewater, $5 \mu g \text{ kg}^{-1}$ dry weight for sediment, and $1.00 \mu g \text{ kg}^{-1}$ wet weight for biota based on previous wide-scope target screening investigations (Diamanti et al., 2020; Gago-Ferrero et al., 2020).

3. Results and discussion

3.1. Compound selection approach

The selection of aliskiren as a compound of potential concern that deserves further monitoring studies was triggered by the NORMAN prioritization scheme, devised to address less-investigated substances for which knowledge gaps are identified. It allocates the substances into

six main action categories on the basis of identified knowledge gaps and required actions. Within each category, the priority is then set using specific indicators: occurrence, hazard (e.g. persistence, bioaccumulation, mobility, endocrine disruption potential) and risk.

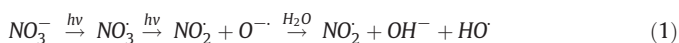
Using this method, aliskiren was selected as a compound of potential interest among a suspect screening list with more than 40,000 substances (SusDat database at 5th September 2019) archived in the NORMAN Digital Sample Freezing Platform (DSFP). Aliskiren molecule was elucidated at level 2A (probable structure by library spectrum match) based on five criteria: *i*) conceivability of the chromatographic retention time; *ii*) mass accuracy; *iii*) isotopic pattern fit; *iv*) number of experimental and predicted fragments; and *v*) percentage of similarity for experimental and library spectra as criteria supporting the tentative identification of the suspects.

To match the prioritization methodology's worst-case scenario approach, the lowest Provisional No Effect Concentration (PNEC) values were used, representing the most conservative ecotoxicological threshold values for suspect compounds. Once no experimental PNEC value for aliskiren was available, it was used the predicted PNEC (P-PNEC) (Aalizadeh et al., 2017). Substances were classified considering: *i*) Frequency of Appearance (FoA), that expresses the percentage of sites where it was detected above the limit of detection (LOD); *ii*) Frequency of PNEC exceedance (FoE), that refers to the percentage of sites where it was detected above the PNEC, and *iii*) the extent of PNEC exceedance (EoE), calculated as the 95th percentile (MEC95) of the substance's maximum observed concentration at each site divided by the P-PNEC. With this approach, aliskiren was prioritized due to "Sufficient frequency of appearance (FoA)". It means a FoA (sites with positive detection) $\geq 20\%$ (42.6% of the investigated wastewater treatment points) 36.5% of those surpassing the predicted PNEC value ($0.041 \mu\text{g L}^{-1}$).

3.2. Aliskiren degradation

The photoinduced degradation of aliskiren was investigated by exposing ultrapure or river water spiked solutions ($5 \mu\text{g L}^{-1}$) to simulated sunlight in order to establish the occurrence of direct and indirect photolysis. Fig. 1a shows that a faster removal occurred in ultrapure water rather than in river water sample, indicating that direct photolysis played an important role in the drug degradation. In particular, aliskiren exhibited a half-life of 24 h in river water, five times higher than in ultrapure water (half-life = 5 h). The decrease rate observed in river water may be due to a scavenging effect played by one or more components of river water, thus hindering the light absorption or quenching the reactive species (Bodhipaksha et al., 2017). Conversely, the degradation of aliskiren is negligible under dark conditions.

It is well-known that dissolved organic matter (DOM) and nitrate act as the main photosensitizer responsible for the formation of reactive species mediating the indirect photolysis (Bodhipaksha et al., 2017; Katagi, 2018; Kim and Zoh, 2013; Mack and Bolton, 1999). For such, we investigated their influence on the photodegradation of aliskiren by performing experiments in MilliQ water in the presence of nitrate or humic acids. The effect of nitrate on the degradation was established by adding 2 mg L^{-1} to ultrapure water, a concentration in the range of those reported for the river water sample under investigation ($1.8\text{--}10 \text{ mg L}^{-1}$) (Marchina et al., 2015) and results are shown in Fig. 1b. The enhanced drug removal can be attributed to the production of $\cdot\text{OH}$ radicals. Hydroxyl radicals can in fact be formed by the absorption of radiation below 350 nm from nitrate in water (Mack and Bolton, 1999), accordingly to the following equation:



Similarly, the role of DOM was investigated by adding humic acids (2 mg L^{-1}) to ultrapure water, in the concentration similar to those observed for the river water sample (Section 2.1) and is reported in Fig. 1b.

DOM addition promotes an inhibitory effect on aliskiren degradation, reasonably due to the combination of a scavenging effect on the radical species produced (Ma and Graham, 1999) and by a competition on the available photons (Andreozzi et al., 2003). DOM is known to induce a controversial effect on the organics removal that is function of the kind of pollutants. Our results are in agreement with the data reported by Martínez-Zapata et al. (Martínez-Zapata et al., 2013) that evidenced an inhibitory effect on the triclosan by the light screening effect of humic acids. Similarly, Chiron et al. (Chiron et al., 2006) reported a faster carbamazepine degradation in Milli-Q water in the presence of nitrate coupled with a slower removal rate in artificial river water with the same nitrate concentration. This effect was attributed to the scavenging effect of $\cdot\text{OH}$ species by the DOM. However, the presence of DOM may also promote the pollutant abatement as observed by Wang et al. (Wang et al., 2017). In wastewater, HA enhanced the removal of caffeine, sulfamethoxazole and diuron, but hindered the degradation of carbamazepine, simazine, triclosan and 2,4-D.

3.2.1. Structural elucidation of aliskiren transformation products

All samples were analyzed by LC-HRMS in ESI positive mode after a pre-concentration step of the sample (see Section 2.2.1) aimed to identify the aliskiren transformation products (TPs). A total of 6 byproducts were identified and data are collected in Table S1, with their m/z ratios, elemental compositions together with retention times and product ions. The putative elemental composition of photoproducts was deduced by the means of Xcalibur software [2.1.0sp1.1160], on the basis of mass accuracy ($<5 \text{ ppm}$) and RDB (ring double bond) index. We searched for potential transformation products on the basis of possible modifications reported in literature (Kotthoff et al., 2020) giving known $\Delta m/z$ differences. A customized searching list was built by software implementation.

Aliskiren fragmentation mechanism was investigated as well by collision-induced dissociation experiments (CID), allowing to establish the most likely losses from the protonated compound (see Fig. 2 and Table S1 for MS^2 and MS^3 fragment list).

Aliskiren MH^+ (m/z 552.4015) fragmented into the products ions at m/z 534 and 436 through the loss of water and $\text{C}_5\text{H}_{12}\text{N}_2\text{O}$, respectively. MS^3 spectrum from the precursor ion at m/z 534 produces four ions: the ions with m/z 517 and 500 through the loss of one (or two) NH_3 molecules, and the product ion at m/z 418 and 401 from the loss of $\text{C}_5\text{H}_{12}\text{N}_2\text{O}$ and the joint loss of $\text{C}_5\text{H}_{12}\text{N}_2\text{O}$ and NH_3 , respectively. MS^3 performed on the ion at m/z 436 fragmented into the ions with m/z 418 and 419 by involving the loss of H_2O and NH_3 , respectively. The observed fragmentation pathways is in agreement with literature data (Kushwah et al., 2018).

Identification level [ES] following the Shymanski approach (Schymanski et al., 2014) was assigned as level 2 for all identified TPs. A compound with m/z 568.3962 and protonated molecular formula $\text{C}_{30}\text{H}_{54}\text{O}_7\text{N}_3^+$ resulted from the monohydroxylation of the parent molecule and is labelled TP6 (see Fig. S1). The precursor ion fragments into m/z 550, 452 and 434 by water loss, loss of $\text{C}_5\text{H}_{12}\text{N}_2\text{O}$ (as observed in parent compound fragmentation) and subsequent H_2O loss, respectively. MS^3 fragmentation performed on the ion at m/z 434 brings to the formation of the structural diagnostic ion at m/z 238, that allowed to confine the hydroxylation in C11 or into the aromatic ring. However, information is not enough to attribute a unique structure.

TP5 with m/z 566.3805 and protonated molecular formula $\text{C}_{30}\text{H}_{52}\text{O}_7\text{N}_3^+$ resulted from TP6 through the oxidation of an alcoholic group into a carbonyl group. Interestingly, TP5 shows the same fragmentation pathways described for TP6. In this case, the product ion at m/z 236 allowed to postulate the oxygen addition in the C11 and to exclude an involvement of the aromatic ring, as shown in the Fig. S2. Therefore, it is reasonable to assess that TP6 holds the OH group on the same carbon.

The transformation product TP4 with m/z 548.3701 and empirical formula $\text{C}_{30}\text{H}_{50}\text{O}_6\text{N}_3^+$ resulted from TP5 through the removal of a

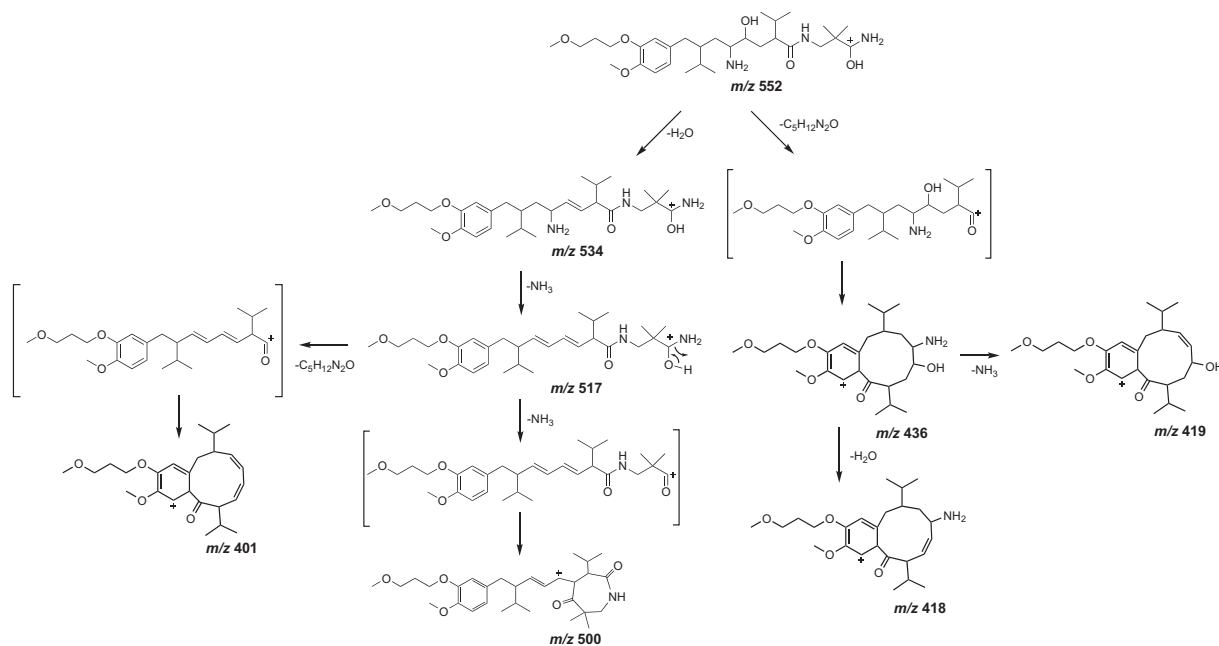


Fig. 2. Fragmentation pathways proposed for the protonated aliskiren molecule.

molecule of water. Dehydrogenation could lead to a double bond between C8 and C9 or between C10 and C11, leading in both cases to stable species. However, the presence of the same fragmentation pathways proposed for TP5 (and TP6) allows proposing the formation of a double bond in C10-C11. Again, the formation of the structural diagnostic ion at m/z 218 supports this hypothesis (see Fig. S3).

The degradation product TP1 with the accurate protonated mass m/z 340.2601 matched with the empirical formula $C_{18}H_{34}O_3N_3^+$ and its formation involved the breakage of the molecule with the loss of the aromatic ring, the cleavage of carbon atom 10 and 11 (see Fig. S4) and a further cyclization. As shown in Fig. S5, the molecular ion fragmented into the ions at m/z 323 and 306 with the loss of one or two molecules of NH_3 . TP1 could result from the photoproduct TP6 with the hydroxyl group addition in the atom C10 (see above).

Additionally, two isomeric forms were found for the ions at m/z 436.3061 matching with the formula $C_{25}H_{42}O_5N^+$ attributed to the cleavage of the amide bond followed by water loss and subsequent cyclization to a lactone for TP2 (Fig. S6) or to lactam for TP3 (Fig. S7). TP2 protonated structure fragmented to form two main product ions: the first one at m/z 346 was originated by the loss of H_2O and tetrahydrofuran (C_4H_6O) and the second one at m/z 419 from the NH_3 loss. The latter fragmented to m/z 387 by the loss of methanol and subsequently to m/z 369 by water loss. Despite structural differences, the TP3 showed similar fragmentation product ions as shown in Fig. S7. These two isomers were previously identified and structurally characterized during stress degradation condition of the drug (Kushwah et al., 2018) and were here distinguished based on the compound polarity. Moreover, TP2 was also reported as an aliskiren human metabolite eliminated by urine and feces (Waldmeier et al., 2007).

3.2.2. Elucidation of aliskiren degradation pathways

Based on the TPs characterized above, we can tentatively suggest the degradation pathways shown in Fig. 3 as the possible photoinduced transformation occurring in river water.

The profile over time for the formed TPs in the different experimental conditions are reported in Fig. S8. Two TPs were detected in the river water sample kept in the dark (namely TP3 and TP5), both showing a delayed formation; this is in line with the marked slowed removal

observed in the dark (see Fig. 1a). Under irradiation, six intermediates were detected in ultrapure water, all showing the maximum intensity at short times, with TP1 only exception.

Five TPs were detected in river water, all showing a disappearance slower than in MilliQ water; in fact, some TPs are still present at the end of the explored time window (72 h). It is also worth pointing out that only one isomer of the photoproduct at m/z 436 was observed in river water (TP3), while two isomers were formed in MilliQ water, as evidenced Table 1.

All the detected TPs were also formed in the presence of nitrate, while only 3 of them were observed in the presence of HA. This can be explained by the differences in the drug removal rate but also by the different reactive species involved in the processes. Moreover, as evidenced in Fig. S8, the nitrate mediated degradation promoted a maximum intensity of intermediates at initial times, in agreement with the fast drug removal. However, longer disappearance of TPs was observed comparing these experiments with the one in ultrapure water. This may be due to the nitrate consumption and the fact that $\cdot OH$ formation is proportional to the nitrate concentration, as shown in Eq. (1).

3.2.3. In silico toxicity estimations

The *in-silico* QSAR predictions on mutagenicity, Fathead minnow, Fish acute and the crustacean *D. Magna* toxicity were considered for aliskiren and its TPs, as reported in Table 2. The mutagenicity prediction, performed using the consensus-based model provides a binary result (positive/negative). Estimations based on this model suggest non-mutagenic properties for all TPs as well as the aliskiren molecule.

The structure-activity relationships simulations using the EPA model predicted the LC50 for the Fathead minnow, which represents the concentration that brings mortality of half of the fish population (*Pimephales promelas*) in 96 h. It was estimated a similar LC50 value for aliskiren and intermediates TP4, TP5 and TP6. Whereas TP2 and TP3 were estimated to be 2.5 and 1.7 more toxic; in the case of TP2, it is reasonably due to the formation of the lactone group as previous reported (Xiao et al., 1996). On the contrary, TP1 was estimated as substantially less toxic ($LC_{50} = 29.67 \text{ mg L}^{-1}$), reasonably due to the breakage of the molecule with the loss of the aromatic ring, vide supra.

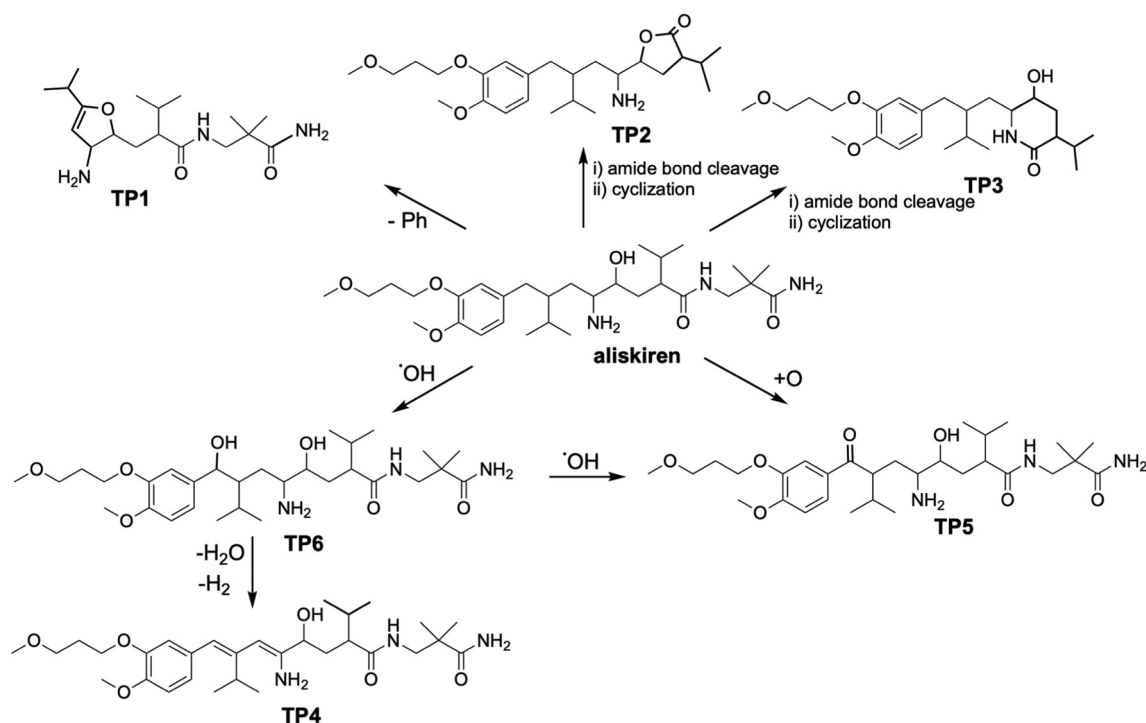


Fig. 3. Photoinduced degradation pathways suggested for aliskiren.

Simulations for the LC50 of Fish acute were predicted with similar concentrations for the majority of TPs and the parent compound, with the exception of TP2 and TP3 that were estimated 9-fold more toxic. Interestingly, these two TPs were formed from the drug cyclization.

Simulations based on EPA model estimated lower inhibitory effect for aliskiren and TP5 (LC50 = 0.03 mg L⁻¹) for the crustaceous compared to the remaining TPs. On the contrary, the TP4 (LC50 = 47.87 mg L⁻¹) was estimated 167-fold less toxic than the parent compound.

Table 1

Summary of aliskiren photoproducts observed in ultrapure water (MQ), river water (RW) in the dark and under irradiation, also in the presence of nitrate and humic acid; (+) observed, (-) non observed.

Compound	Degradation conditions				
	MQ	RW - photolysis	RW - dark	Nitrate	Humic acid
TP1	+	+	-	+	+
TP2	+	-	-	+	-
TP3	+	+	+	+	+
TP4	+	+	-	+	+
TP5	+	+	+	+	-
TP6	+	+	-	+	-

Table 2

Toxicity values estimated using the VEGA software for aliskiren and TPs.

Compound	Mutagenicity	Fathead minnow LC50 (96 h) (mg L ⁻¹)	Fish acute LC50 (48 h) (mg L ⁻¹)	<i>D. Magna</i> LC50 (48 h) (mg L ⁻¹)
Aliskiren	Negative	2.15	8.88	0.03
TP1	Negative	29.67	7.46	0.23
TP2	Negative	0.84	0.11	0.08
TP3	Negative	1.24	0.10	0.24
TP4	Negative	2.24	8.81	47.87
TP5	Negative	2.96	9.10	0.03
TP6	Negative	5.63	9.13	0.51

3.2.4. Retrospective analysis

The results of the screening as regards frequency of appearance (FoA) are presented in Table 3. Two out of the screened TPs were detected in the samples, while three TPs (TP2, TP4 and TP5) were not detected in any sample. The highest FoA was observed for wastewater (either influent or effluent). More specifically, aliskiren's highest FoA (43%) was observed in effluent wastewater, TP1's highest FoA (32%) was observed in influent wastewater and TP3's highest FoA (32%) was observed in influent wastewater. Aliskiren was detected only in wastewater (influent and effluent), whereas TP1 and TP3 were also detected in other matrices, what can suggest the drug degradation through the formation of TPs with higher persistence. Both TPs were detected in surface waters (river and seawater), in fresh water sediments and in biota. However, TP3 was detected sporadically at samples other than wastewater, having FoA below 6% for all investigated matrices. Overall, the TP1 proved to have the most wide-spread occurrence, what is in agreement with the higher abundance among other TPs observed during the degradations experiments in river water experiments (see Section 3.2). Therefore, TP1 was detected in surface water (FoA 23%) and in

Table 3

Frequency of appearance (FoA; ranged between 0 and 1) of aliskiren and its TPs in various environmental samples. Substances that were not detected are marked as "N.D."

Environmental matrix	N° of screened samples	Aliskiren	TP1	TP2	TP3	TP4	TP5
Influent wastewater	120	0.22	0.32	N.D.	0.32	N.D.	N.D.
Effluent wastewater	126	0.43	0.06	N.D.	0.22	N.D.	N.D.
River	78	N.D.	0.23	N.D.	0.01	N.D.	N.D.
Seawater	105	N.D.	0.21	N.D.	0.02	N.D.	N.D.
Groundwater	7	N.D.	N.D.	N.D.	N.D.	N.D.	N.D.
Biota coastal	101	N.D.	0.09	N.D.	0.02	N.D.	N.D.
Biota river	71	N.D.	N.D.	N.D.	0.03	N.D.	N.D.
Biota terrestrial	52	N.D.	N.D.	N.D.	N.D.	N.D.	N.D.
Biota marine	62	N.D.	0.02	N.D.	0.07	N.D.	N.D.
Sediment river and marine	32	N.D.	0.19	N.D.	0.09	N.D.	N.D.

sediments (FoA 19%). None of the compounds were detected in ground-water samples. The detection of TP1 and TP3 in various matrices even at low detection rates, highlights the importance of transformation mechanisms that take place in the environment. As shown in Section 3.2.3, TP1 was predicted as less or with similar toxicity of aliskiren, while TP3 was estimated with higher toxicity than the parent compound (with exception of *D. magna*). These results highlight that the aliskiren degradation mechanism may yield TPs of unknown behavior and toxicity that should be accessed by bioassays to target and non-targeted organism.

4. Conclusions

The degradation pathways followed by aliskiren in natural water were elucidated by spiking river water with drug concentrations close to those detected in natural samples, and they proceeded with the formation of six photoproducts, structurally elucidated through LC-HRMS. The drug transformation involved monohydroxylation, oxidation and breakage of the molecule. Additionally, under simulated sunlight it was shown that nitrate at environmental concentrations can promote a faster degradation of aliskiren, while humic substances had a negative impact. Retrospective suspect screening performed on environmental samples revealed the formation of two TPs detected during the laboratory-scale experiments in several environmental matrices. It is noteworthy that one of them (TP3) exhibits a toxicity higher than aliskiren toward Fathead minnow and fish, so raising concern about its potential harmful impact. The information about the aliskiren degradation and TPs here elucidated will enhance the NORMAN network databases, intended to exchange CECs data, to support stakeholders and regulatory agencies to take preventive measurements to preserve the water quality.

CRedit authorship contribution statement

Nuno P.F. Gonçalves: Investigation, Writing – original draft, Writing – review & editing. **Lucia Iezzi:** Investigation. **Masho H. Belay:** Investigation. **Valeria Dulio:** Conceptualization, Formal analysis. **Nikiforos Alygizakis:** Writing – review & editing, Formal analysis. **Federica Dal Bello:** Data curation, Formal analysis. **Claudio Medana:** Methodology, Validation. **Paola Calza:** Conceptualization, Methodology, Funding acquisition.

Declaration of competing interest

The authors declare that they have no known competing financial interests or personal relationships that could have appeared to influence the work reported in this paper.

Acknowledgements

This work is part of a project that has received funding from the European Union's Horizon 2020 research and innovation programme under the Marie Skłodowska-Curie Grant Agreement No 765860 (AQUALITY).

Authors acknowledge the contributors of samples to the NORMAN Digital Sample Freezing Platform (DSFP). Authors are thankful to the research group of Prof. Nikolaos S. Thomaidis. Moreover, authors acknowledge the efforts of Dr. Jaroslav Slobodnik and his research team to expand the sample deposited in DSFP.

Appendix A. Supplementary data

Supplementary data to this article can be found online at <https://doi.org/10.1016/j.scitotenv.2021.149547>.

References

- Aalizadeh, R., von der Ohe, P.C., Thomaidis, N.S., 2017. Prediction of acute toxicity of emerging contaminants on the water flea *Daphnia magna* by ant Colony optimization-support vector machine QSTR models. *Environ. Sci. Process. Impacts* 19, 438–448. <https://doi.org/10.1039/c6em00679e>.
- Alygizakis, N.A., Besselink, H., Paulus, G.K., Oswald, P., Hornstra, L.M., Oswaldova, M., Medema, G., Thomaidis, N.S., Behnisch, P.A., Slobodnik, J., 2019a. Characterization of wastewater effluents in the Danube River basin with chemical screening, in vitro bioassays and antibiotic resistant genes analysis. *Environ. Int.* 127, 420–429. <https://doi.org/10.1016/j.envint.2019.03.060>.
- Alygizakis, N.A., Oswald, P., Thomaidis, N.S., Schymanski, E.L., Aalizadeh, R., Schulze, T., Oswaldova, M., Slobodnik, J., 2019b. NORMAN digital sample freezing platform: a European virtual platform to exchange liquid chromatography high resolution-mass spectrometry data and screen suspects in "digitally frozen" environmental samples. *TrAC Trends Anal. Chem.* 115, 129–137. <https://doi.org/10.1016/j.trac.2019.04.008>.
- Alygizakis, N.A., Urík, J., Beretsou, V.G., Kampouris, I., Galani, A., Oswaldova, M., Berendonk, T., Oswald, P., Thomaidis, N.S., Slobodnik, J., Vrana, B., Fatta-Kassinos, D., 2020. Evaluation of chemical and biological contaminants of emerging concern in treated wastewater intended for agricultural reuse. *Environ. Int.* 138, 105597. <https://doi.org/10.1016/j.envint.2020.105597>.
- Andreozzi, R., Marotta, R., Paxéus, N., 2003. Pharmaceuticals in STP effluents and their solar photodegradation in aquatic environment. *Chemosphere* 50, 1319–1330. [https://doi.org/10.1016/S0045-6535\(02\)00769-5](https://doi.org/10.1016/S0045-6535(02)00769-5).
- Benfenati, E., Mangano, A., Gini, G., 2013. VEGA-QSAR: AI inside a platform for predictive toxicology. *CEUR Workshop Proc.* 1107, 21–28.
- Berg, S.M., Whiting, Q.T., Herrli, J.A., Winkels, R., Wammer, K.H., Remucal, C.K., 2019. The role of dissolved organic matter composition in determining photochemical reactivity at the molecular level. *Environ. Sci. Technol.* 53, 11725–11734. <https://doi.org/10.1021/acs.est.9b03007>.
- Bodhipaksha, L.C., Sharpless, C.M., Chin, Y.P., MacKay, A.A., 2017. Role of effluent organic matter in the photochemical degradation of compounds of wastewater origin. *Water Res.* 110, 170–179. <https://doi.org/10.1016/j.watres.2016.12.016>.
- Bodrato, M., Vione, D., 2014. APEX (Aqueous photochemistry of environmentally occurring Xenobiotics): a free software tool to predict the kinetics of photochemical processes in surface waters. *Environ. Sci. Process. Impacts* 16, 732–740. <https://doi.org/10.1039/c3em00541k>.
- Boulard, L., Dierkes, G., Schlüsener, M.P., Wick, A., Koschorreck, J., Ternes, T.A., 2020. Spatial distribution and temporal trends of pharmaceuticals sorbed to suspended particulate matter of german rivers. *Water Res.* 171, 115366. <https://doi.org/10.1016/j.watres.2019.115366>.
- Bu, Q., Shi, X., Yu, G., Huang, J., Wang, B., 2016. Assessing the persistence of pharmaceuticals in the aquatic environment: challenges and needs. *Emerg. Contam.* 2, 145–147. <https://doi.org/10.1016/j.emcon.2016.05.003>.
- Chiron, S., Minero, C., Vione, D., 2006. Photodegradation processes of the antiepileptic drug carbamazepine, relevant to estuarine waters. *Environ. Sci. Technol.* 40, 5977–5983. <https://doi.org/10.1021/es060502y>.
- Diamanti, K.S., Alygizakis, N.A., Nika, M.C., Oswaldova, M., Oswald, P., Thomaidis, N.S., Slobodnik, J., 2020. Assessment of the chemical pollution status of the Dniester River basin by wide-scope target and suspect screening using mass spectrometric techniques. *Anal. Bioanal. Chem.* 412, 4893–4907. <https://doi.org/10.1007/s00216-020-02648-y>.
- Duggan, S.T., Chwieduk, C.M., Curran, M.P., 2010. Aliskiren: a review of its use as monotherapy and as combination therapy in the management of hypertension. *Drugs* <https://doi.org/10.2165/11204360-000000000-00000>.
- Ebele, A.J., Abou-Elwafa Abdallah, M., Harrad, S., 2017. Pharmaceuticals and personal care products (PPCPs) in the freshwater aquatic environment. *Emerg. Contam.* 3, 1–16. <https://doi.org/10.1016/j.emcon.2016.12.004>.
- Gago-Ferrero, P., Bletsou, A.A., Damalas, D.E., Aalizadeh, R., Alygizakis, N.A., Singer, H.P., Hollender, J., Thomaidis, N.S., 2020. Wide-scope target screening of >2000 emerging contaminants in wastewater samples with UPLC-Q-ToF-HRMS/MS and smart evaluation of its performance through the validation of 195 selected representative analytes. *J. Hazard. Mater.* 387, 121712. <https://doi.org/10.1016/j.jhazmat.2019.121712>.
- Godoy, A.A., Kummrow, F., Pamplin, P.A.Z., 2015. Occurrence, ecotoxicological effects and risk assessment of antihypertensive pharmaceutical residues in the aquatic environment - a review. *Chemosphere* 138, 281–291. <https://doi.org/10.1016/j.chemosphere.2015.06.024>.
- Hollender, J., van Bavel, B., Dulio, V., Farmen, E., Furtmann, K., Koschorreck, J., Kunkel, U., Krauss, M., Munthe, J., Schlabach, M., Slobodnik, J., Stroomborg, G., Ternes, T., Thomaidis, N.S., Togola, A., Tornero, V., 2019. High resolution mass spectrometry-based non-target screening can support regulatory environmental monitoring and chemicals management. *Environ. Sci. Eur.* 31. <https://doi.org/10.1186/s12302-019-0225-x>.
- Katagi, T., 2018. Direct photolysis mechanism of pesticides in water. *J. Pestic. Sci.* 43, 57–72. <https://doi.org/10.1584/jpestics.D17-081>.
- Kim, M.K., Zoh, K.D., 2013. Effects of natural water constituents on the photo-decomposition of methylmercury and the role of hydroxyl radical. *Sci. Total Environ.* 449, 95–101. <https://doi.org/10.1016/j.scitotenv.2013.01.039>.
- Kothhoff, L., O'Callaghan, S.L., Lisec, J., Schwerdtle, T., Koch, M., 2020. Structural annotation of electro- and photochemically generated transformation products of moxidecin using high-resolution mass spectrometry. *Anal. Bioanal. Chem.* 412, 3141–3152. <https://doi.org/10.1007/s00216-020-02572-1>.
- Kushwah, B.S., Gupta, J., Singh, D.K., Kurmi, M., Sahu, A., Singh, S., 2018. Characterization of solution stress degradation products of aliskiren and prediction of their

- physicochemical and ADMET properties. *Eur. J. Pharm. Sci.* 121, 139–154. <https://doi.org/10.1016/j.ejps.2018.05.021>.
- Libiseller, G., Dvorzak, M., Kleb, U., Gander, E., Eisenberg, T., Madeo, F., Neumann, S., Trausinger, G., Sinner, F., Pieber, T., Magnes, C., 2015. IPO: a tool for automated optimization of XCMS parameters. *BMC Bioinf.* 161 (16), 1–10. <https://doi.org/10.1186/S12859-015-0562-8> (2015).
- Liška, I., Wagner, F., Sengl, M., Deutsch, K., Slobodník, J., Paunovic, M., 2021. Joint Danube Survey 4 Scientific Report: A Shared Analysis of the Danube River. Vienna.
- Loos, M., Hollender, J., Schymanski, E.L., Ruff, M., Singer, H.P., 2012. Bottom-up peak grouping for unknown identification from high-resolution mass spectrometry data. *ASMS 2012 Annual Conference Vancouver, Oral Session Informatics: Identification*.
- Luo, Z., Tseng, M.Y., Minakata, D., Bai, L., Hu, W.P., Song, W., Wei, Z., Spinney, R., Dionysiou, D.D., Xiao, R., 2021. Mechanistic insight into superoxide radical-mediated degradation of carbon tetrachloride in aqueous solution: an in situ spectroscopic and computational study. *Chem. Eng. J.* 410, 128181. <https://doi.org/10.1016/j.cej.2020.128181>.
- Ma, J., Graham, N.J.D., 1999. Degradation of atrazine by manganese-catalysed ozonation: influence of humic substances. *Water Res.* 33, 785–793. [https://doi.org/10.1016/S0043-1354\(98\)00266-8](https://doi.org/10.1016/S0043-1354(98)00266-8).
- Ma, J., Minakata, D., O'Shea, K., Bai, L., Dionysiou, D.D., Spinney, R., Xiao, R., Wei, Z., 2021. Determination and environmental implications of aqueous-phase rate constants in radical reactions. *Water Res.* 190, 116746. <https://doi.org/10.1016/j.watres.2020.116746>.
- Mack, J., Bolton, J.R., 1999. Photochemistry of nitrite and nitrate in aqueous solution: a review. *J. Photochem. Photobiol. A Chem.* 128, 1–13. [https://doi.org/10.1016/S1010-6030\(99\)00155-0](https://doi.org/10.1016/S1010-6030(99)00155-0).
- Marchina, C., Bianchini, G., Natali, C., Pennisi, M., Colombani, N., Tassinari, R., Knoeller, K., 2015. The Po river water from the Alps to the Adriatic Sea (Italy): new insights from geochemical and isotopic (d18O-dD) data. *Environ. Sci. Pollut. Res.* 22, 5184–5203. <https://doi.org/10.1007/s11356-014-3750-6>.
- Martínez-Zapata, M., Aristizábal, C., Peñuela, G., 2013. Photodegradation of the endocrine-disrupting chemicals 4n-nonylphenol and triclosan by simulated solar UV irradiation in aqueous solutions with Fe(III) and in the absence/presence of humic acids. *J. Photochem. Photobiol. A Chem.* 251, 41–49. <https://doi.org/10.1016/j.jphotochem.2012.10.009>.
- Maszkowska, J., Stolte, S., Kumirska, J., Lukaszewicz, P., Mioduszewska, K., Puckowski, A., Caban, M., Wagil, M., Stepnowski, P., Bialk-Bielinska, A., 2014. Beta-blockers in the environment: part II. Ecotoxicity study. *Sci. Total Environ.* 493, 1122–1126. <https://doi.org/10.1016/j.scitotenv.2014.06.039>.
- Meringer, M., Schymanski, E.L., 2013. Small molecule identification with MOLGEN and mass spectrometry. (2013). *Metab* 3, 440–462. <https://doi.org/10.3390/METABO3020440> 3, 440–462.
- Miller, T.H., Bury, N.R., Owen, S.F., MacRae, J.I., Barron, L.P., 2018. A review of the pharmaceutical exposome in aquatic fauna. *Environ. Pollut.* 239, 129–146. <https://doi.org/10.1016/j.envpol.2018.04.012>.
- Naciones Unidas, 2018. United Nations Secretary-General's Plan: Water Action Decade 2018–2028, p. 25.
- Network, N., Aalizadeh, R., Alygizakis, N., Schymanski, E., Slobodnik, J., Fischer, S., Cirka, L., 2020. SO | SUSDAT | Merged NORMAN Suspect List: SusDat. <https://doi.org/10.5281/ZENODO.3900203>.
- NORMAN Database System, 2020. NORMAN Database System URL <https://www.norman-network.com/nds/> (accessed 7.30.20).
- Patel, M., Kumar, R., Kishor, K., Misra, T., Pittman, C.U., Mohan, D., 2019. Pharmaceuticals of emerging concern in aquatic systems: chemistry, occurrence, effects, and removal methods. *Chem. Rev.* 119, 3510–3673. <https://doi.org/10.1021/acs.chemrev.8b00299>.
- Santos, L.H.M.L.M., Araújo, A.N., Fachini, A., Pena, A., Delerue-Matos, C., Montenegro, M.C.B.S.M., 2010. Ecotoxicological aspects related to the presence of pharmaceuticals in the aquatic environment. *J. Hazard. Mater.* 175, 45–95. <https://doi.org/10.1016/j.jhazmat.2009.10.100>.
- Schymanski, E.L., Jeon, J., Gulde, R., Fenner, K., Ruff, M., Singer, H.P., Hollender, J., 2014. Identifying small molecules via high resolution mass spectrometry: communicating confidence. *Environ. Sci. Technol.* <https://doi.org/10.1021/es5002105>.
- Singer, H.P., Wössner, A.E., McArdell, C.S., Fenner, K., 2016. Rapid screening for exposure to “non-target” pharmaceuticals from wastewater effluents by combining HRMS-based suspect screening and exposure modeling. *Environ. Sci. Technol.* 50, 6698–6707. <https://doi.org/10.1021/acs.est.5b03332>.
- Slobodnik, J., Alexandrov, B., Komorin, V., Mikaelyan, A., Guchmanidze, A., Arabidze, M., Korshenko, A., 2017. National Pilot Monitoring Studies and Joint Open Sea Surveys in Georgia.
- Stankiewicz, A., Giebultowicz, J., Stankiewicz, U., Wroczynski, P., Nalecz-Jawecki, G., 2015. Determination of selected cardiovascular active compounds in environmental aquatic samples - methods and results, a review of global publications from the last 10 years. *Chemosphere* 138, 642–656. <https://doi.org/10.1016/j.chemosphere.2015.07.056>.
- Tautenhahn, R., Böttcher, C., Neumann, S., 2008. Highly sensitive feature detection for high resolution LC/MS. *BMC Bioinf.* 9, 504. <https://doi.org/10.1186/1471-2105-9-504>.
- von der Ohe, P.C., Dulio, V., 2013. NORMAN Prioritisation Framework for Emerging Substances.
- Waldmeier, F., Glaenzel, U., Wirz, B., Oberer, L., Schmid, D., Seiberling, M., Valencia, J., Riviere, G.J., End, P., Vaidyanathan, S., 2007. Absorption, distribution, metabolism, and elimination of the direct renin inhibitor aliskiren in healthy volunteers. *Drug Metab. Dispos.* 35, 1418–1428. <https://doi.org/10.1124/dmd.106.013797>.
- Wang, Y., Roddick, F.A., Fan, L., 2017. Direct and indirect photolysis of seven micropollutants in secondary effluent from a wastewater lagoon. *Chemosphere* 185, 297–308. <https://doi.org/10.1016/j.chemosphere.2017.06.122>.
- Xiao, H., Madhyastha, S., Marquardt, R.R., Li, S., Vodala, J.K., Frohlich, A.A., Kempainen, B.W., 1996. Toxicity of ochratoxin a, its opened lactone form and several of its analogs: structure-activity relationships. *Toxicol. Appl. Pharmacol.* 137, 182–192. <https://doi.org/10.1006/taap.1996.0071>.